THERMAL-HYDRAULIC ANALYSIS FOR LIQUID METAL FALLING FILM IN AN IFE FIRST WALL PROTECTION SYSTEM

Alice Y. Ying and Mohamed A. Abdou

Mechanical, Aerospace and Nuclear Engineering Department
6288 Boelter Hall
University of California, Los Angeles
Los Angeles, CA 90024-1597
310-206-8815

ABSTRACT

Thermal-hydraulic fluid flow analyses have been performed for a wetted wall concept for an IFE reactor. The lead film on the first wall SiC surface is supplied partly by injection from the top of the upper hemisphere and partly by seepage through the first wall cooling channels. The analyses indicate that to maintain the film on the hemispheric surface, there are minimum film velocity and thickness requirements. These film thicknesses (~ 6 mm) might be too high to achieve a high repetition rate through conduction heat removal. In order to use the convective heat removal, it requires that the film surface temperature should be low enough to have a significant amount of condensation. The present calculation indicates that this is possible if the pressure requirement for the cavity is higher than 10^{-2} torr.

INTRODUCTION

A wetted wall concept using a thin liquid (Pb) film for the cavity design has been proposed for the PROMETHEUS study[1]: an inertial fusion energy (IFE) reactor study led by McDonnell Douglas. Previous studies using this concept for IFE first wall protection[2,3] helped in optimizing the design in related to the film formation. The purpose of this work is to present thermal-hydraulic calculations and help define the operating parameters using this concept for PROMETHEUS reactor. These parameters include film flow characteristics with associated heat removal mechanism, the fluid injection and seepage rates, and the effect of time dependent cavity pressure.

In this concept, similar to the SENRI-II study,[3] the film which coats the first wall surface of the cylindrical reactor chamber is initiated by a nozzle injector located at the top end cap. The inertia of the jet is adequate to provide coverage on the entire surface without dripping into the cavity. This nozzle injector is exposed to the microexplosion and therefore, should be accessible for replacement, as needed. In addition, some amount of flow is added to the film by seepage through the fibrous first wall coolant channel. The seepage flow helps to maintain a good coverage; however, the amount of flow should be kept as small as possible to prevent destabilizing the film. The film flows down the vertical section of the first wall and ultimately reaches the drain. A schematic view of film flow system is illustrated in Figure 1.

The minimum required film thickness is determined from the evaporation caused by target explosions. This depends on the target energy spectrum, yields, absorption characteristics of the film material and vapor radiation processes. The depth of evaporation was estimated to be about 10 μm per shot.[1] This amount of film will be condensed back on the film before the next shot. While under ideal conditions only 10 μm is needed, additional thickness is allowed for nonuniformities and extra margin.

FILM FLOW ANALYSIS

The fluid leaves the injector and flows along the surface. The film flow is driven mainly by gravity, which is then balanced by the drag along the wall and the flow accelerational force. The force balances in the normal and tangential directions for an incompressible fluid element shown schematically in Figure 2 can be written as:

$$\rho \frac{V^2}{r_v} \delta = -\frac{2\sigma\cos(\theta)}{R} - \frac{2\sigma}{r_v} + \rho g_c \delta \sin(\theta) \qquad (1)$$

$$V\delta\frac{\partial V}{\partial l} = g_c \delta\cos(\theta) - \tau_D \qquad (2)$$

where ρ is the fluid density, V is the liquid film velocity in the tangential (flow) direction, δ is the film thickness, r_v is radius of curvature, R is the local radius, σ is the surface tension, g_c is the gravity acceleration, τ_D is the wall friction force exerted on the fluid along the flow direction, θ is the

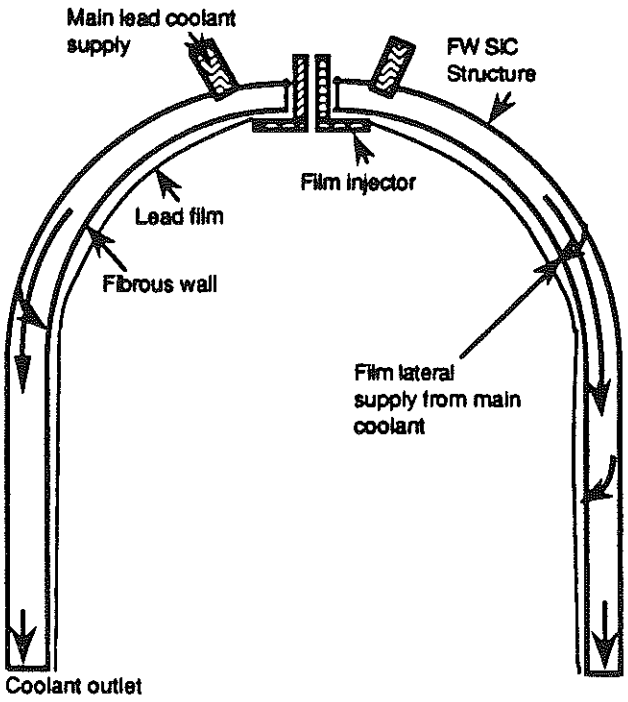

Figure 1 Schematic View of film flow system

angle that the tangent to the fluid element forms with the z axis, and l is the distance measured along the flow direction.

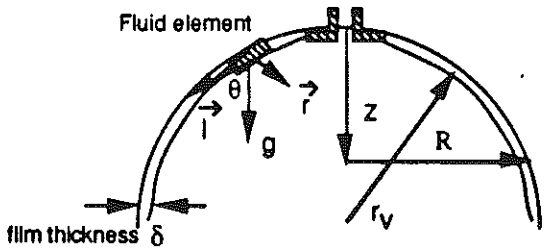

Figure 2 Illustration of force elements acting on the upper wall film

Another equation for the film flow is the conservation of mass, which is written as:

$$\frac{\partial VA}{\partial l} = q^* \qquad (3)$$

where A = film cross-sectional flow area, and q* is the seepage inflow rate per unit length. The lateral inflow rate is determined from the lateral supply rate based on Darcy's equation and is:

$$q^* = v\, A_l \qquad (4)$$

where A_l is the lateral flow area per unit flow length and v is seepage velocity and is discussed under the section of flow through fibrous wall.

Before solving for film velocities and thicknesses, two important constraints must be considered: (1) attachment of the film to the wall so that the hole for the laser beam is not covered, (2) the influence of film flow characteristics on the protection of the wall by maintaining a minimum film thickness.

(1) Requirement for Attachment to the Wall

The film velocity in the upper end cap must be sufficiently high such that the film remains attached to the surface. The solution of equation (1) indicates that at different locations on the curved surface, there is a minimum velocity required to prevent the fluid separating from the wall for film thickness greater than 10 μm. Figure 3 shows these minimum required velocities as a function of distance away from the upper hemispherical cap. The calculations are performed for a radius of 5 meters. The minimum velocity decreases as flow proceeds downstream; the highest minimum velocity is 7 m/sec. With this minimum velocity and the film thickness for X-ray and debris absorption (~100 μm), the fluid appears to be turbulent, with Reynolds number (Re) larger than critical film Reynolds number (1600).

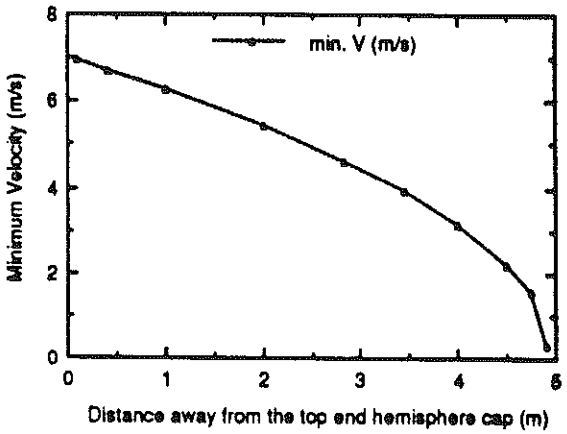

Figure 3. Minimum required film velocity for film attaching on the upper hemisphere wall as a function of distance away from the top

(2) Turbulent Film Characteristics and Minimum Film Thickness

A number of previous studies have explored the wave structure of a vertical turbulent falling film.[4,5] These studies indicate that the wave structure is complex - there appear to be several classes of waves and each class has certain random features. Waves formed at the film interface appear to be a combination of large waves with small ripples superimposed on the large waves. Film waviness is

complicated further by variations in both the instantaneous and the time-averaged values of film thickness with film travel. An illustration of turbulent wave structure is shown in Figure 4,[4] which indicates that various film thicknesses can be observed in this type of film. While using this turbulent liquid film for the first wall protection, the concern is whether a minimum film thickness can be greater than the required film thickness for X-ray and debris protection(such as 100 μm). Experimental study of Takahama[5] shows that the minimum film thickness decreases towards the entrance region; however, at a greater distance the minimum film thickness becomes almost constant independent of Re and the longitudinal distance (It is noticed that the Reynolds number defined in Takahama's study is one fourth of the Reynolds number defined in the present paper.). The minimum film thicknesses identified in their study were about 300 μm. Figure 5 illustrats their results of film thickness variations along the longitudinal direction.

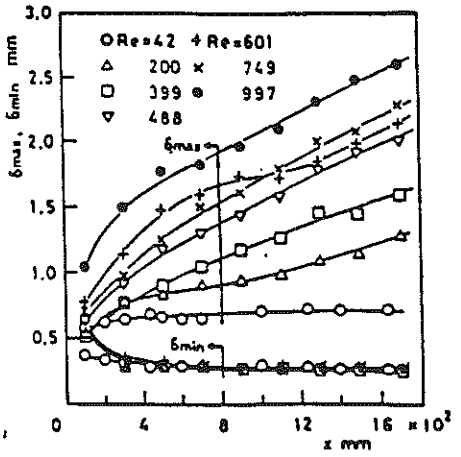

Figure 5 Longitudinal distributions of maximum and minimum film thicknesses

WALL FRICTIONAL DRAG

To solve the aforementioned film flow equations, an expression is needed for the wall drag which appears in equation 2. In general, the turbulent wall friction force is expressed in terms of the friction factor, f, as:

$$\tau_D = \frac{f}{4\delta}\frac{V^2}{2g_c} \tag{5}$$

For Reynolds number less than 100,000, the friction factor (f) given by the Blasius formula[6] provides the closest estimation of turbulent film thickness when compared to the empirical correlation of turbulent falling film thickness(δ_t) presented by Gimbutis.[7]

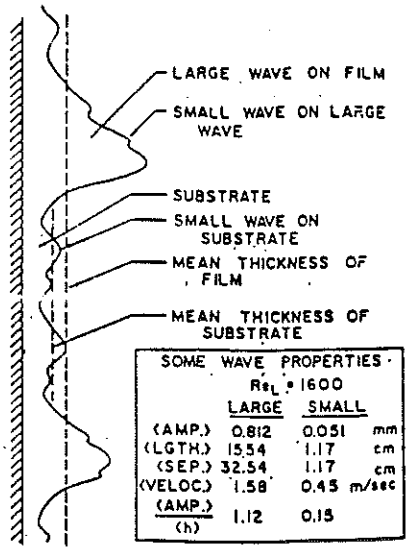

Figure 4 Illustration of turbulent film wave structures

The Blasius formula for friction factor (f) is given as:

$$f = \frac{0.316}{Re^{0.25}} \tag{6}$$

and the Gimbutis' turbulent film thickness is expressed as:

$$\delta_t = 0.136\left(\frac{\nu_f}{g_c}\right)^{1/3} Re^{0.583} \tag{7}$$

where the Reynolds number (Re) is defined as

$$Re = \frac{4V\delta\rho}{\mu_f} \tag{8}$$

The turbulent film thickness and volumetric flow rate at different locations on the curved hemispheric wall based on the Gimbutis's formula are estimated for the minimum required velocities from Fig. 2. The results are shown in Figure 6. They indicate that to maintain the flow attached to the surface, the film thickness will be greater than 6.4 mm. The minimum volumetric flow rate increases first, reaches a peak value and decreases as the flow proceeds to downstream locations. If a thin film is a desirable design option, the injection could be minimized with flow continuously added to the film to satisfy the minimum required flow rate criterion. After the required peak flow rate is achieved, a thinner film can be obtained by extracting the flow from the film. Once the film travels to the straight portion of the cavity wall, there is no minimum film velocity required.

FLOW THROUGH POROUS, FIBROUS WALL

In the PROMETHEUS design, some amount of the fluid is continuously added to the film from the cooling channels lying behind the porous, fibrous wall, through which the coolant seeps onto the surface facing the explosion due to the pressure difference between the cooling system and the cavity. This cooling system is to provide the necessary flow rate to remove the first wall thermal power. The lead coolant enters the fibrous cooling tube at the upper end cap with an inlet temperature and pressure of 375 °C and 1 MPa, respectively. The upper temperature of lead is set at 525 °C to avoid the corrosion problem in the heat transport loop. The amount of lead needed for removing the first wall thermal power of 1357.7 MW is equal to 5.87×10^4

Kg/s. The average lead velocity in a 5 cm diameter cooling tube is 4.8 m/s. The lead coolant pressure along the flow channel is estimated from:

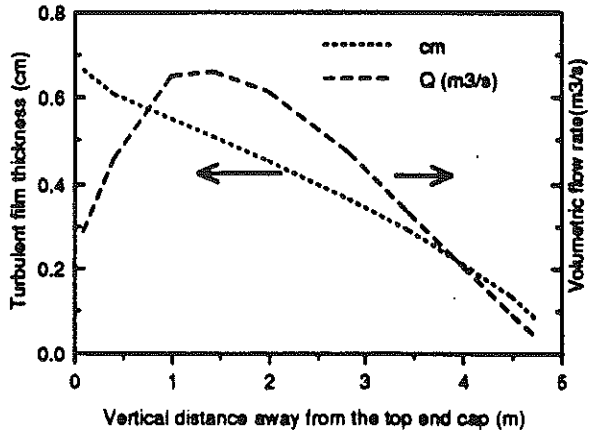

Figure 6 Turbulent film thickness and minimum volumetric flow rate for attaching on the hemisphere wall as a function of vertical distance from the top

$$P(Z) = P(Z-\Delta Z) - f\frac{\rho V^2}{2}\frac{l}{D_h} + \rho\, g_c\, \Delta Z \qquad (9)$$

where P(Z) is the pressure at vertical Z location, f is the friction factor and is obtained from the Moody diagram with a relative roughness of 0.001, V is the coolant velocity, l is the coolant flow path, D_h is the equivalent hydraulic diameter, and ΔZ is the vertical distance. The calculated coolant pressure as a function of Z is shown in Figure 7.

The flow through the porous fibrous medium is estimated by Darcy's formulation:[9]

$$0 = -\Delta P - \frac{\mu}{\kappa} v\, \delta_w \qquad (10)$$

where v is the average seepage velocity of inflow from the coolant through the fibrous tube wall, ΔP is the pressure difference between the coolant and the film, μ is the dynamic viscosity of the fluid, κ is the permeability and δ_w is the fibrous wall thickness. Equation (10) indicates that the permeability of the porous tube could be tailored to provide optimum flow control. In the present analysis, the permeability is calculated from:

$$\kappa = \frac{d^2}{175}\frac{\varepsilon^3}{(1-\varepsilon)^2} \qquad (11)$$

where d = fiber pore diameter and ε is the porosity.[9] It should be noticed that the amount of seepage flow rate should not be so high as to impart momentum into the film and cause film detachment. The seepage flow rate as a function of Z for a permeability of 1.76×10^{-14} m^2 is shown in Figure 7.

RESULTS OF FILM FLOW ANALYSIS

Equations 2 and 3 were solved for the film thickness and film velocity along the flow direction for different initial flow rates and wall characteristics. Example results are shown in Figures 8 for film thickness characteristics and Figure 9 for film velocity behavior.

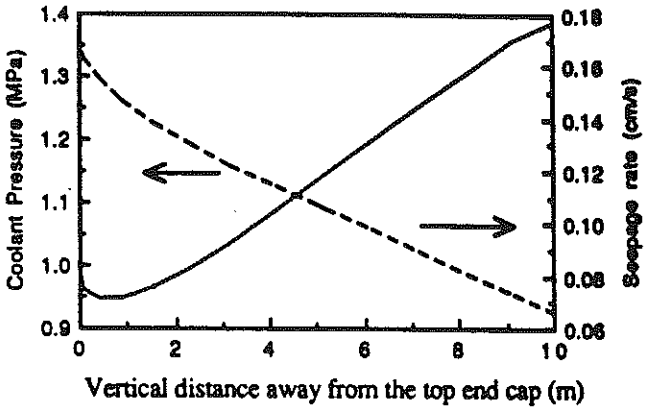

Figure 7 Coolant pressure and seepage rate as a function of distance away from the top end cap

There are several parameters which affect the film characteristics. These are injection angle, film injection velocity and initial film thickness, wall permeability and lateral supply rate. Two cases were analyzed: Case 1 has a relatively modest injection velocity of 15 m/s with a relatively thick film of 1.15 cm and in Case 2, the injection velocity increases to 40 m/s with film thickness reduced to 0.43 cm. For both cases, the film flow is initiated by injecting the flow at an angle of 82° (defined as the angle between the flow and the gravity directions) with a wall permeability of 1.764×10^{-14} m^2. A decrease of injection angle means a larger surface is exposed to the explosion. Although this might soften the requirement for the attachment, this would introduce maintenance complications.

Beyond the injector region there is little difference between the two cases. In each case, the velocity decreases immediately due to the wall drag. The film thickness increases first due to the reduction of film velocity and decreases later because of the expansion of the flow area. The maximum film thickness decreases from 1.9 to 1.6 cm as the injection velocity increases from 15 to 40 m/s. For both cases, the final film thicknesses are about 0.6 cm.

These film thicknesses are much thicker than that required for the X-ray and debris absorption and may be too thick for removing heat by conduction mechanism. To reduce the film thickness on the curved hemispheric wall, the

flow can be extracted out of the film through tailoring the first wall once the flow reaches the peak point. In addition, the lateral supply from the lead cooling system can be reduced by decreasing the wall permeability for this purpose.

CONVECTIVE HEAT TRANSFER USING FILM FLOW

The analysis of film flow on the upper hemisphere indicates that maintaining a film smaller than a few mm is not possible. As the film thickness grows, heat removed by conduction is reduced. This would not be desirable because a high repetition rate would not be possible. This section is to explore using the film for first wall heat removal, in addition to wall protection.

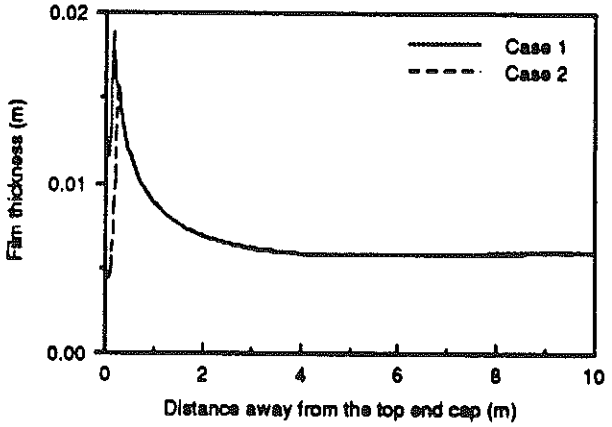

Figure 8 Film thicknesses as a function of vertical distance away from the top end cap

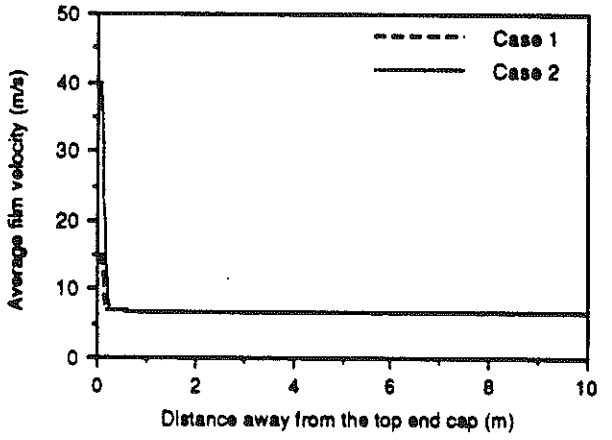

Figure 9 Average film velocity behavior as a function of distance away from the top end cap

Calculations based on the energy balance indicate that a volumetric flow rate of 5.87×10^4 Kg/s is needed to limit the coolant bulk temperature rise of 125 C. For this amount of flow rate, analyses are performed for two different cases. In Case 1, the flow injection rate at the top end cap is maximized, and the porosity of the wall is 10%. In Case 2, the lateral supply rate is maximized by increasing the wall porosity to 30 %. Here, the coolant lying behind the fibrous first wall serves as a neutron multiplier and a coolant reservoir.

The total amounts of flow from the lateral supply for cases 1 and 2 are 4% and 35% of the ultimate flow rate, respectively. At these cases, the lateral momentum flux are only a few % of the longitudinal momentum flux, so that 1-D analysis should be adequate.

Results are shown in Figures 10 and 11. The film flow is initiated by injecting the flow at an angle of 82° (about 10 cm away from the end point). Initial velocities of 35 and 40 m/s, and initial film thicknesses of 4 and 2.5 cm are assumed for cases 1 and 2, respectively.The results show that in each case, the velocity decreases very rapidly initially due to wall drag. The film thickness first increases due to the reduction of film velocity and then decreases later because of the increase in the flow area. For case 1, the peak film thickness is 5.38 cm and the final film thickness is 1.54 cm. For case 2, the peak mean film thickness is about 3.9 cm and the final mean film thickness is about 1.6 cm. If the initial velocity can be further increased, a more uniform mean film thickness can be obtained.

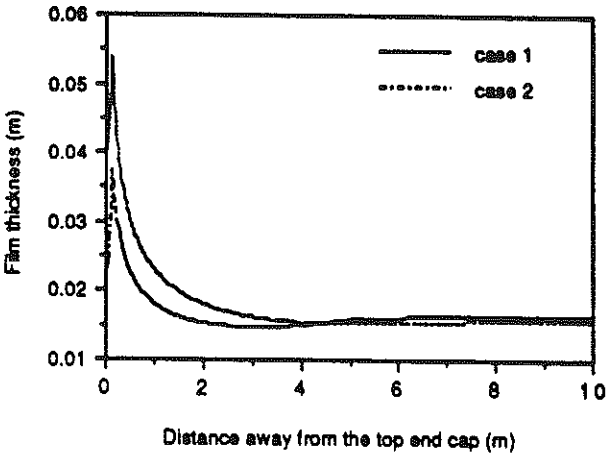

Figure 10 Film thicknesses as a function of distance away from the top end cap

The concerns of using a couple of cm thick film are whether the temperature on the first wall is beyond the design limit and whether the temperature on the film surface is too high for condensation to take place. The pressure and temperature relationship of lead is illustrated in Figure 12.[9] At pressure of 1×10^{-3} torr, the saturation temperature is about 627 °C, the saturation temperature increases to 838 °C as the pressure increases to 1×10^{-2} torr. In order to have a significant amount of condensation on the film surface, the film surface temperature should be less than 627 °C for

laser driven IFE and 838 °C for heavy ion driven IFE. The film heat transfer coefficient given by Lee[10] is examined for this purpose. The turbulent film heat transfer coefficient for liquid metal is of the same order as the laminar heat transfer coefficient. The non-dimensional laminar heat transfer coefficient for condensation was expressed in terms of Reynolds number and written as:

$$\left(\frac{v_f^2}{g_c}\right)^{1/3} \frac{h_{av}}{k} = 1.47\ Re^{-1/3} \qquad (12)$$

At Reynolds number of 8.5×10^5, which corresponds to the Reynolds number at the vertical section of the reactor chamber, the heat transfer coefficient is estimated as 1.51×10^4. For a heat flux of 2.7×10^6 w/m^2, the film temperature drop is about 200 °C, this gives the maximum film surface temperature of 725 °C.

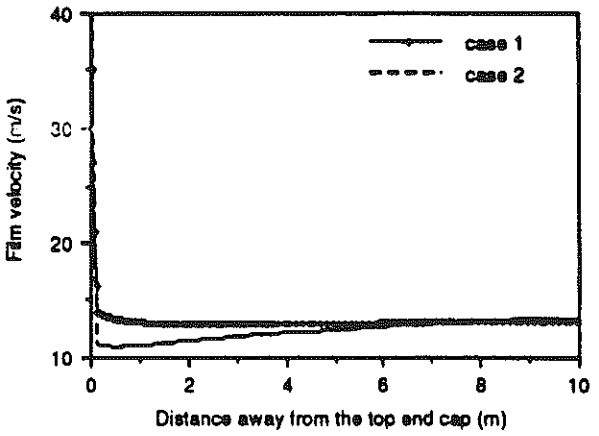

Figure 11 Film velocities as a function of vertical distance away from the top end cap

The first wall surface temperature can be estimated by the turbulent heat transfer coefficient at the wall from the Colburn correlation ,[11] which is stated as:

$$\frac{h}{k}\left[\frac{\mu^2}{\rho^2 g_c}\right]^{1/3} = 0.056\ Re^{0.2}\left(\frac{C_p \mu}{k}\right)^{1/3} \qquad (13)$$

The estimation of film temperature gradient based on the turbulent heat transfer coefficient predicted from the aforementioned equation and heat flux of 2.7×10^6 w/m^2 is about 10 °C.

Although these preliminary calculations indicate that the film surface is cold enough for condensation to take place in a heavy ion driven IFE cavity and the first wall surface temperature is low, further analysis on the cavity clearing and liquid metal turbulent film heat transfer coefficient for condensation are needed to demonstrate that this concept is feasible.

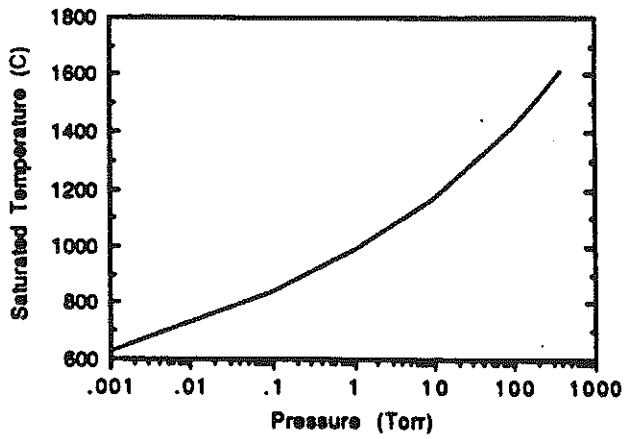

Figure 12 Saturation temperature as a function of pressure for lead liquid metal

EFFECT OF TIME-DEPENDENT CAVITY PRESSURE

Once an explosion occurs, some of the lead film is vaporized and increases the cavity pressure. Under these circumstances, lead may be pushed back into the cooling channels, and the film will thin, slow down, and possibly become dry at the wall. In addition, the reactive impulse due to vaporized liquid and cavity shock waves may cause the same phenomenon, as well as disrupting the film surface. Here, the transient behavior of film velocity and film thickness due to cavity pressure build-up are examined. The effect of impulsive loading is beyond the scope of this work.

It is assumed that the pressure difference between the main coolant and the cavity can be expressed as:

$$\Delta P = P_{inlet} - 0.5 \times 10^6 \times \left(1.-e^{\left(-\frac{time}{3\tau}\right)}\right) \qquad (14)$$

where τ (= 0.25 s) is the time interval between the explosions. Figure 11 shows the assumed cavity pressure and pressure difference histories at the uppermost point of the cavity. The above equation does not attempt to simulate the real cavity pressure. The peak cavity overpressure was estimated < 0.1 MPa.[10] (The cavity pressure at 0.25 seconds following the mircoexplosion falls below 1 mm torr.)

The fluid transient behavior can be described by:

Transient Darcy's equation:

$$\rho \frac{\partial v}{\partial t} = -\frac{\partial P}{\partial y} + \frac{\mu}{\kappa} v \qquad (15)$$

Transient film momentum equation:

$$\frac{\partial V}{\partial t} = -V \frac{\partial V}{\partial l} + g_c \cos(\theta) - \tau_D \qquad (16)$$

Example results of ultimate film thickness and velocity histories following the cavity pressure build-up is shown in Figure 12. The case shown is for initial jet velocity and film

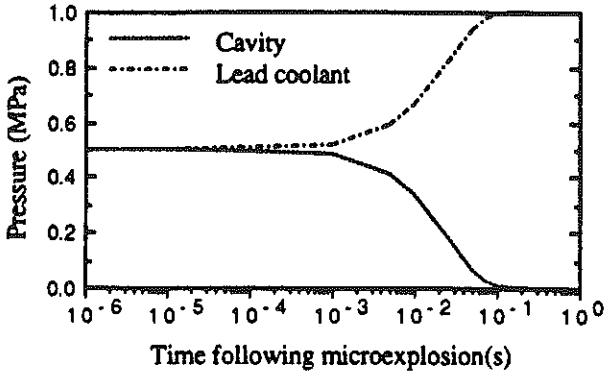

Figure 13 Cavity and differential pressure histories at the uppermost point of the cavity

thickness of 20 m/s and 0.9 cm, respectively. The calculations indicate that the film velocity tends to decrease and might drop to the level that the film separation from the wall occurs if the initial jet velocity is not high enough. For the case shown, the film approaches to asymptotic (steady state) behavior at about 0.2 seconds following the cavity pressure build-up.

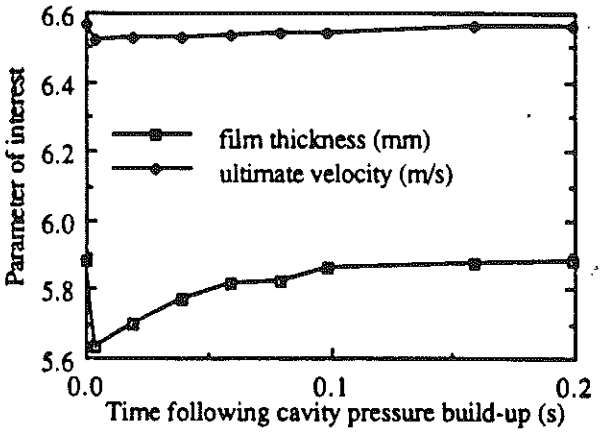

Figure 14 Ultimate film thickness and film velocity histories following the cavity pressure build-up

ADDITIONAL CONCERNS OF USING FILM FLOW AS FIRST WALL PROTECTION

Although thin film flow provides attractive features for first wall protection, there are several technical issues remaining to be investigated to asses the feasibility of this concept.[12] These include: 1) wetting characteristics of the lead on the SiC (used as first wall structure) material, 2) flow on inverted surfaces, 3) problems in providing uniform coverage over large engineering structures, 4) flow past obstacles, such as beam peneration, 5) stability of the film subjected to pressure impulse, 6) integrity of porous composite SiC material which is immersed in lead metal and subjected to a high radiation environment, and 7) consequences of dry spots.

SUMMARY

The analyses indicate that a very thin film (< 1 mm) is not obtainable on the inverted surface without causing film separation from the surface. (There is no limitation on the minimum film thickness on the vertical surface.) To reduce the film thickness, the film needs to be accelerated along the flow direction. Possible accelerating mechanisms include: (1) reducing the wall drag, and/or (2) inducing an MHD pump action in the film along the flow direction. Simple scaling analysis for achieving a thin film using a magnetic field was performed by Chao and Tillack.[13]

The possibility of using convective heat removal was explored. The use of laminar heat transfer coefficient for condensation indicates that the film surface temperature is low enough to allow a significant amount of condensation for the heavy ion driven IFE. However, the condensation rate might not be adequate for the laser driven IFE due to a more restricted cavity pressure requirement. Further analyses of cavity clearing and modeling of liquid metal heat transfer coefficient for condensation are needed to demonstrate its feasibility. Under external perturbations, such as cavity pressure buildup, the time-dependent film flow analysis indicates that the transient effect results in an increase of injection rate to prevent the film from breaking down. This further thickens the film and reduces the conduction heat removal efficiency.

Acknowledgement

This work was performed under MCMSC Purchase Order YOE416R. The suggestions provided by Dr. Mark Tillack at UCLA are very much appreciated.

Nomenclature

A	film cross-sectional flow area
A_l	lateral flow area per unit length
C_p	specific heat
D_h	equivalent hydraulic diameter
d	fiber pore diameter
f	friction factor
g_c	gravity acceleration
h	turbulent heat transfer coefficient
h_{av}	average heat transfer coefficient for condensation
k	thermal conductivity
l	distance along the flow direction
P	pressure
q^*	seepage inflow rate per unit length
R	local radius
Re	Reynolds number
r_v	radius of curvature

V film flow velocity
v seepage velocity
t time
y radial direction
Z vertical distance

Greek letter

ρ density
σ surface tension
θ angle tangent to the fluid element forms with z axis
δ film thickness
δ_w first wall thickness
ν kinematic viscosity
μ viscosity
κ permeability
ε porosity
τ time interval between the explosions
τ_D wall friction force

Sub-Indices

f fluid
t turbulent

References

1. M. S. TILLACK et al., "Initial Design of the PROMETHEUS Wetted Wall IFE Reactor Cavity," UCLA-FNT-51, October (1991).

2. L. A. BOOTH, "Central Station Power Generation By Laser-Driven Fusion," Nuclear Engineering and Design 24, (1973) 263-313.

3. N. NAKAMURA et al., "Conceptual Design Study on Inertial Confinement Reactor "SENRI-II"," Nuclear Technology/Fusion, Vol. 4, 854, September (1983).

4. K. J. CHU and A. E. DUKER, "Statistical Characteristics of Thin, Wavy Films: Part II. Studies of the Substrate and its Wave Structure," AIChE J., Vol. 20, No.4, 695 (1974).

5. H. TAKAHAMA and S. KATO, "Longitudinal Flow Characteristics of Vertically Falling Liquid Films Without Concurrent Gas Flow," Int. J. Multiphase Flow, Vol. 6, pp. 203-215 (1980).

6. R. H. FRENCH, Open-Channel Hydraulics, McGraw-Hill, New York, 1985.

7. G. GIMBUTIS, "Heat Transfer for a Turbulent Falling Film," Proc. 5th Int. Heat Transfer Conf., Tokyo, Japan, Vol. 2, pp. 85-89 (1974).

8. S. ERGUN "Fluid Flow Through Packed Columns," Chemical Engineering Prog., 48, 89(1952).

9. R. N. LYON, Liquid Metal Handbook: Chapter 3:Liquid Metals Physical Properties, NAVEXOS P-733 (Rev.), Atomic Energy Commission, Department of the Navy, Washington, D.C., June, 1952.

10. JON LEE, "Turbulent Film Condensation," A.I.Ch. E. L, p. 540 July (1964)

11. J. G. COLLIER, Convective Boiling and Condensation, Second edition, McGraw-Hill, New York, 1972, pp. 330-332.

12. M. S. TILLACK et al., "Final Report of IFE Reactor Design Studies: Chapter 6.8 Cavity Design and Analysis," Draft, Feburary, 1992.

13. T. C. H. CHAO and M. S. TILLACK, "Evaluation of Alternatives to Avoid Dripping of Liquid Lead at the Upper End Cap in an IFE Reactor Cavity," UCLA-IFNT-8, October 1991.